Solid State Ionics 354 (2020) 115401

Contents lists available at ScienceDirect

Solid State Ionics

journal homepage: www.elsevier.com/locate/ssi

Structure, hydration, and proton conductivity in 50% La and Nd doped CeO_2 – $La_2Ce_2O_7$ and $Nd_2Ce_2O_7$ – and their solid solutions

Liv-Elisif Kalland[a,*], Andreas Løken[a,b], Tor S. Bjørheim[a], Reidar Haugsrud[a], Truls Norby[a]

[a] Centre for Materials Science and Nanotechnology, Department of Chemistry, University of Oslo, FERMiO, Gaustadalléen 21, NO-0349 Oslo, Norway
[b] Jotun Performance Coatings, Jotun A/S, NO-3202 Sandefjord, Norway[1]

ARTICLE INFO

Keywords:
TG-DSC
C-type structure
Fluorite structure
Hydration
Proton conductivity
Vacancy ordering

ABSTRACT

We have measured water uptake and hydration enthalpy in 50% La and Nd doped CeO_2, also to be taken as compositions in the series $La_{2-x}Nd_xCe_2O_7$ (x = 0.0, 0.5, 1.0 and 2.0) using combined thermogravimetry (TG) and differential scanning calorimetry (DSC), TG-DSC. The TG-DSC data unambiguously yield standard molar hydration enthalpies of ~−74 kJ/mol independent of water uptake. The interpretation of the TG results, however, does not fit a classical model of hydration of all oxygen vacancies. Instead, the hydration appears to be limited to a small fraction of the free vacancies. Hydration further decreases as the Nd content (x) and long-range order increases and regions of disorder decrease. We propose a new model explaining why hydration occurs only in a small fraction of the nominally free vacancies: The higher basicity of La/Nd compared to Ce promotes protonation at oxide ion sites with high coordination to La/Nd, and the observed water uptake and modelling suggests that mainly oxide ions fully coordinated to 4 La/Nd neighbours become protonated. The statistical variation of coordination around oxygen sites in a disordered fluorite oxide creates a limited number of such oxide ions sites which results in limited hydration. The model matches well the experimental results and DFT calculations of proton trapping at the fully La-coordinated sites for 50% La-doped CeO_2, and also rationalizes conductivity data.

1. Introduction

$Ln_2Ce_2O_7$ with Ln = La or other large lanthanides is sometimes referred to as 50% lanthanide-doped ceria since the structure remains related to the cubic ceria parent structure [1–3]. Adhering to the Kröger-Vink notation, the doping reaction can then be written as:

$$Ln_2O_3 = 2Ln'_{Ce} + 3O^{\times}_{O} + v^{\bullet\bullet}_{O} \quad (1)$$

This results in 1 oxygen vacancy per formula unit $Ln_2Ce_2O_7$. The structure may as such potentially incorporate one molecule of water, i.e., two protons, per vacancy if the material is fully hydrated:

$$H_2O_{(g)} + O^{\times}_{O} + v^{\bullet\bullet}_{O} = 2OH^{\bullet}_{O} \quad (2)$$

In support of this, $La_2Ce_2O_7$, which exhibits oxide ion conductivity in the dry state, has been reported to hydrate and exhibit proton conduction in the presence of water vapour [2]. From reaction (2) it is evident that a lower stability (higher energy) of the oxygen vacancy, or a higher stability (lower energy) of the hydroxide species, will result in more favourable hydration thermodynamics [4,5]. Hydration enthalpies in oxides can range from endothermic values such as in undoped ceria [6] to highly exothermic for a wide range of oxides including rare earth sesquioxides [7,8], pyrochlores [9], and perovskites [10,11].

High concentrations of defects, for instance by high doping levels, can induce a number of defect-defect interactions, and corresponding associates will affect the concentrations of free defects, the degree of hydration, and the apparent mobility of defects. These can comprise vacancy-vacancy pairs, vacancy-dopant pairs, vacancy-double dopant clusters, proton-dopant pairs and clusters, and long-range order of vacancies and dopant-vacancy constellations. Accordingly, lanthanide-doped ceria (Ln-CeO_2) shows a steep decrease in the oxide ion conductivity when doping levels increase above 10–20 mol% [1,3,12,13]. While ceria with moderate acceptor doping levels exhibits negligible protonation and bulk proton conductivity [5], ceria heavily doped with some large lanthanides, such as 50% La-doping corresponding to $La_2Ce_2O_7$, can be hydrated and shows significant proton conductivity at lower temperatures in wet atmospheres [2,14]. This we may qualitatively attribute to the higher basicity of the large lanthanides, notably La and Nd, relative to that of Ce.

* Corresponding author.
E-mail address: l.e.kalland@kjemi.uio.no (L.-E. Kalland).
[1] Current affiliation.

https://doi.org/10.1016/j.ssi.2020.115401
Received 19 December 2019; Received in revised form 18 June 2020; Accepted 29 June 2020
Available online 04 August 2020

When comparing previous studies we find that the oxide ion conductivity, amount of hydration, and proton conductivity all decrease from $La_2Ce_2O_7$ to $Nd_2Ce_2O_7$ [2,14–16]. Structural investigations in the $La_{2-x}Nd_xCe_2O_7$ system showed indications of increasing long-range ordering of oxygen vacancies from La to Nd (increasing x) [17]. Ordering increases the stability of oxygen vacancies and one may expect this to affect the amount of water uptake through the compositional series investigated here.

Here, we investigate how the high doping level (basicity) and ordering impact hydration by a study of the water uptake and thermodynamics of hydration in the $La_{2-x}Nd_xCe_2O_7$ series (x = 0.0, 0.5, 1.0 and 2.0) using combined thermogravimetry and differential scanning calorimetry (TG-DSC), as well as electrical characterization. We compare the thermodynamic parameters obtained by fitting the water uptake data from TG-DSC to the classical model for acceptor doped oxides as described by for example Kreuer [10], and the results from measuring the hydration enthalpy directly by combined TG-DSC as demonstrated by Kjølseth et al. [11]. Conductivity measurements performed in wet and dry atmospheres determine the contribution of proton conductivity for the series. The observed levels of hydration and hydration enthalpies are discussed in relation to long-range structural order through the series and a new approach to local site and coordination energetics as a result of high doping levels.

2. Experimental details

Combined thermogravimetry (TG) and differential scanning calorimetry (DSC), TG-DSC, were conducted on powder samples with the compositions $La_{2-x}Nd_xCe_2O_7$ (x = 0.0, 0.5, 1.0, and 2.0). The powders were prepared by solid state reaction and heat treated in several cycles with a final temperature of 1400 °C yielding almost phase pure samples based on Rietveld analysis of long scan powder X-ray diffraction data (XRD). The Rietveld analysis determined the impurities to be 0.05 wt% of $La_{9.33}(SiO_4)_6O_2$ in the $La_2Ce_2O_7$ sample and 0.002–0.004 wt% of Nd_2O_3 in the Nd containing samples. Moreover, the structure of the samples was characterized using XRD and neutron powder diffraction (ND), and analysed using Rietveld and the reverse Monte Carlo method. For detailed descriptions of sample preparation, XRD and ND, and interpretations thereof, see [17].

TG-DSC measurements were performed using a Netzsch Simultaneous Thermal Analyzer (STA 449C Jupiter) connected to a water vapour generator providing an atmosphere of pH_2O = 1 atm. The powder samples were dried at 1000 °C for 60 min and thereafter equilibrated in dry N_2 (or O_2 for two of the measurement series) at the given temperature prior to the hydration by introduction of steam. The background was determined running an empty crucible under identical conditions and the background was subtracted from the measurements. Fig. 1 shows examples of DSC and TG curves upon hydration for the different compositions at 250 °C. The water uptake is determined from the mass change, while the heat exchange associated with the water uptake is extracted by integration of the DSC signal using a sigmoidal shape to account for the baseline shift. By dividing the heat exchange by concentration of water, we obtain the hydration enthalpy ΔH_{hydr} per mole of H_2O at the given temperature.

Before we turn to results, we mention two possible complications of the measurements, and how we have addressed them. First, since compositions containing high levels of Nd have been suggested to take up some oxygen under oxidizing conditions [15] due to the slight tendency of Nd^{3+} to be oxidized to Nd^{4+}, hydration measurements for $LaNdCe_2O_7$ and $Nd_2Ce_2O_7$ are also conducted in O_2 for comparison. We do not find significantly different water uptakes in O_2 vs N_2, and conclude therefore that oxidation does not affect the defect structure significantly, i.e., electron holes are minority defects.

Secondly, the measured water uptake for the end member $Nd_2Ce_2O_7$ is particularly low, and chemisorbed water or the formation of hydroxide phases of the Nd_2O_3 impurity phase could in principle account for a significant part of the total water uptake. Based on preliminary BET studies and estimates of the amount of Nd_2O_3 from XRD, the maximum water uptake from these would correspond to 0.007 and 0.012–0.024 mol H_2O per mol oxide, respectively. We rule out a major effect of hydroxide formation because at the fixed high water vapour pressure we apply, this should manifest itself as steps in the TG curve. Our data exhibit no steps, but rather a behaviour resembling hydration of an acceptor doped oxide as seen in many works (e.g. [10]). Based on this the measurements for $Nd_2Ce_2O_7$ will be discussed assuming that the mass changes are due to hydration, although we cannot rule out the possibility that adsorption and hydroxide formation influence the data for this compound.

Electrical characterization was carried out on pellets made by pressing the same powders as used for structural characterization using a 20 mm die, at 125 MPa pressure. All samples were sintered at 1400 °C for 5 h, heated with a ramp rate of 300°/h, and cooled with a ramp rate of 140°/h. After sintering the samples exhibited a relative density of approximately 60%. Electrodes were made by painting three layers of

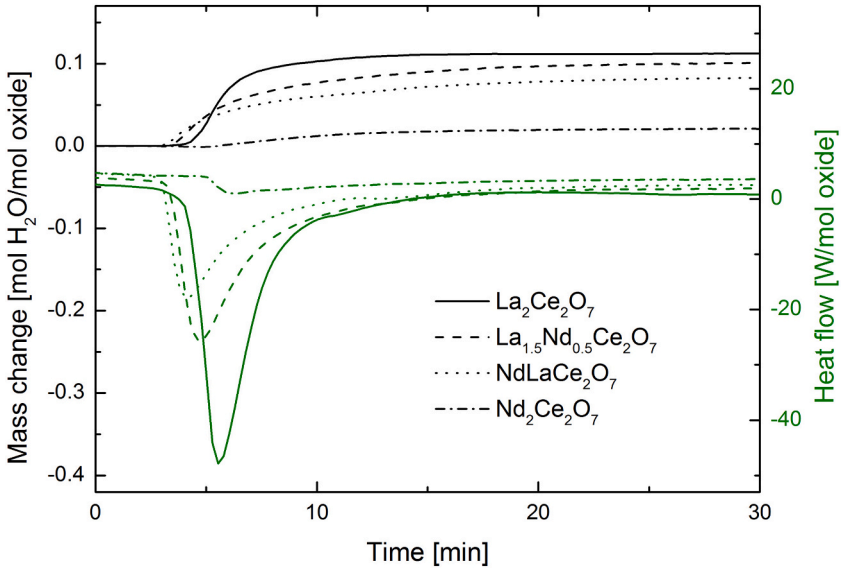

Fig. 1. TG and DSC curves upon hydration (pH_2O = 1 atm) at 250 °C for $La_{2-x}Nd_xCe_2O_7$ with x = 0.0, 0.5, 1.0 and 2.0.

platinum ink (Metalor Pt-ink 6926) on each side of the samples and dried. A Pt grid was added with the last Pt-layer, and the electrode was finally annealed according to the ink specifications.

Electrical characterization was performed by using a 2-point 4 wire setup mounting the samples in a ProboStat™ (NORECS, Norway) and connected to an impedance spectrometer (Solartron 1260 FRA). The conductivity data reported are measured at 10 kHz while impedance sweeps were recorded for some conditions covering the experimental window to ensure that the constant frequency conductivities reflect bulk properties.

3. Results and discussion

3.1. Water uptake and thermodynamic values

Fig. 2 shows the water uptake for each composition based on the relative mass changes measured by TG-DSC (squares). All the compositions hydrate to some extent. This can be taken to be hydration of a nominally undoped oxide by introduction of two defects, for instance oxygen interstitials and protons, or it can be taken to represent hydration of oxygen vacancies present to charge compensate acceptor dopants, as described above. In any case, the expected maximum hydration is the same in the $Ln_2Ce_2O_7$ series, corresponding to one mole of water per mole of oxide. However, attempts to fit the data to this model with a fixed maximum hydration level of 1 mol/mol oxide result in very poor fits, even when using data only above 250 °C. The fitted standard hydration entropies are reasonable (of the order of −130 J/mol K) but the standard hydration enthalpies in the order of −40 to −50 kJ/mol are, as we shall see later, much less negative than corresponding values from TG-DSC, which are of the order of −70 kJ/mol. Hence, this model appears inapplicable and is not pursued further here.

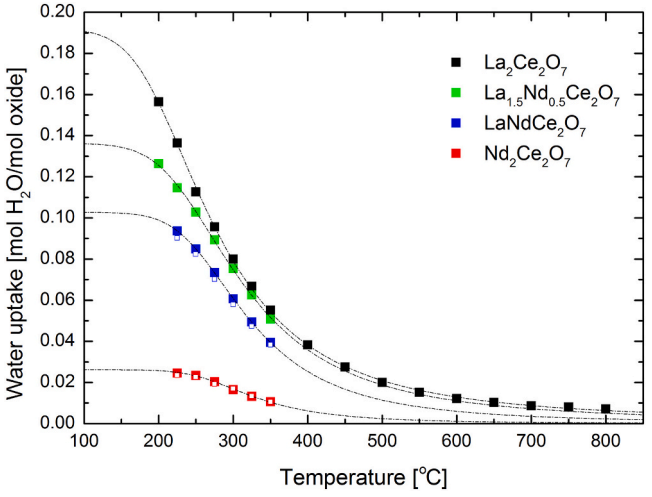

Fig. 2. Measured water uptake for each of the compositions (solid and open squares, respectively, for N_2 and O_2 atmospheres) along with curve-fitted lines based on a defect chemical model with variable effective acceptor level and corresponding maximum water uptake appearing as the plateaus at low temperatures.

Instead, we analyse the data in a first approach according to a model where the maximum hydration is a variable quantity which we fit to the data along with the standard entropy and enthalpy of hydration. We solve three equations, namely the equilibrium coefficient for the reaction in Eq. (2),

$$K_{Hydr} = \exp\left(-\frac{H^\circ_{hydr}}{RT}\right)\exp\left(\frac{S^\circ_{hydr}}{R}\right) = \frac{[OH^\bullet_O]^2}{[v^{\bullet\bullet}_O][O^\times_O]p_{H_2O}} \quad (3)$$

the constancy of the sum of charges from available oxygen vacancies and hydroxide ions, corresponding to an effective variable acceptor level (a model used earlier in similar studies of acceptor doped oxides [18,19]),

$$[Acc'_{eff}] = 2[v^{\bullet\bullet}_O] + [OH^\bullet_O], \quad (4)$$

and the oxide ion site balance made up from effectively neutral structural empty oxygen sites, available charged oxygen vacancies, and hydroxide ions,

$$[O^\times_O] = 8 - ([v^\times_O] + [v^{\bullet\bullet}_O] + [OH^\bullet_O]) \quad (5)$$

where the three variables ΔH°_{hydr}, ΔS°_{hydr} and $[v_O^{\bullet\bullet}]$ are the standard hydration enthalpy and entropy and the molar concentration of available, or free, oxygen vacancies, respectively. In this approach, the neutral (structural) empty oxygen sites vary between 1 per formula unit for a fully ordered system and 0 for a fully disordered one, expressed by the level of effective acceptors; $[v^\times_O] = 1 - \frac{1}{2}[Acc'_{eff}]$. The molar concentration of protons $[OH_O^\bullet]$ is given by the measured water uptake $[OH_O^\bullet] = 2[H_2O]$ (from Eq. (2)), and p_{H_2O} is set to the value used for the hydration isobars, namely 1 atm.

Resulting saturation levels, enthalpies and entropies are listed in Table 1 along with the standard deviation resulting from the curve fitting. The modelled curves corresponding to the derived parameters are included in Fig. 2.

When analysing the combined TG-DSC data we obtain a mean value and standard deviation when comparing the evaluated enthalpies for each temperature within a specified temperature range. The extracted molar enthalpies of hydration and the standard deviation (based on the difference between results at different temperatures) are included in Table 1 and Fig. 3. The uncertainty of the extracted parameters increases with increasing temperature and Nd-content, as the water uptake and accompanying heat exchange diminish. The data point at 350 °C, which forms an outlier enthalpy, is hence omitted when calculating the mean values for $Nd_2Ce_2O_7$.

The mean standard enthalpies of hydration determined by TG-DSC are remarkably similar for all the compositions, with an average value of −74 kJ/mol, however there seems to be a trend of decreasingly exothermic hydration enthalpies with increasing content of Nd. The same parameter extracted from fitting the measured water uptake (see Table 1) with a variable saturation limit comes out at qualitatively

Table 1
Thermodynamic values from fitting of the measured water uptake and the extracted hydration enthalpies from TG-DSC. The uncertainties reflect standard deviation based on the data sets averaged and curve-fitted. Actual uncertainties including systematic errors will be larger.

Compound	Hydration parameters fitted to a model with limited effective acceptor level and water uptake saturation			Enthalpies from TG-DSC
	Saturation level [mol H_2O/mol $Ln_2Ce_2O_7$]	ΔS°_{hydr} [J/mol K]	ΔH°_{hydr} [kJ/mol]	ΔH°_{hydr} [kJ/mol] (200–350 °C)
$La_2Ce_2O_7$	0.191 ± 0.004	−128 ± 1	−57 ± 1	−77 ± 3
$La_{1.5}Nd_{0.5}Ce_2O_7$	0.136 ± 0.002	−134 ± 4	−63 ± 2	−74 ± 3
$LaNdCe_2O_7$	0.1027 ± 0.0005	−157 ± 1	−76 ± 1	−73 ± 3
$Nd_2Ce_2O_7$	0.0260 ± 0.0006	−188 ± 10	−89 ± 6	−72 ± 12

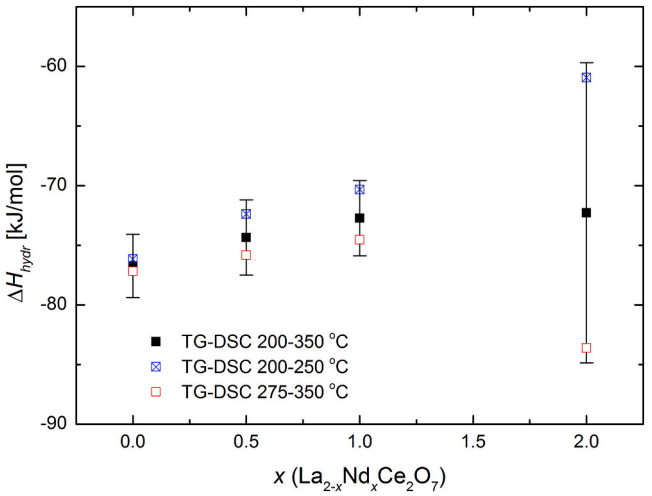

Fig. 3. Average enthalpies from TG-DSC as a function of x for all temperatures (black) with std. error and for temperatures above and below 250 °C (red 275–350 °C, blue 200–250 °C).

similar values, but the correlation between the three fitted parameters is large and the uncertainties are much bigger than those from the fitting statistics alone.

In comparison with the hydration enthalpy of approximately −77 kJ/mol for $La_2Ce_2O_7$ determined by TG-DSC in this work, Besikiotis et al. [2] reported −90 kJ/mol for the same material and method. However, they used a much lower p_{H_2O} = 0.025 atm, yielding lower changes in sample mass and heat flow upon hydration, i.e. larger uncertainties than in our current study. The hydration enthalpy of −80 kJ/mol obtained by Besikiotis et al. [2] by curve fitting of water uptake from TG is disregarded here because they assumed full hydration contrary to our observation of limited and variable maximum hydration, to be discussed in the next section.

The standard entropies of hydration extracted from fitting water uptake average at approximately −150 J/mol K, and are within the range of entropies typically found for hydration of oxides (−120 ± 40 J/mol K) [5].

In addressing the deviation between the hydration enthalpies determined directly by TG-DSC and by curve-fitting presented in Table 1, it is first important to recognize the major differences in the derivation of the two sets of thermodynamic data. The TG-DSC measurements directly reflect the enthalpies associated with the overall process in the materials when exchanging the surrounding atmosphere from dry to wet gas, whereas the TG data relies on curve fitting, carrying assumptions of a defect model representing hydration and with potentially correlated fitting parameters. However, fitting TG data as a function of temperature may serve to determine first approximated values of the saturation level for the different compositions. All in all, the standard molar hydration thermodynamic parameters take on rather consistent and reasonable values. Hence, the major parameter of interest remains the small and variable hydration limit, which we shall discuss further in the following.

3.2. Limited hydration of the heavily doped disordered fluorites – a new model

The fitted maximum levels for water uptake are far from the theoretical limit of 1 mol/mol $Ln_2Ce_2O_7$, indicating that the water uptake is thermodynamically limited to lower values, suggested from the experimental results to be around 0.2 (20%) in the case of $La_2Ce_2O_7$. Is there a way we can plausibly rationalize such a low maximum hydration of the nominally available oxygen vacancies in the disordered heavily doped, or oxygen deficient, fluorite structure as found in $La_2Ce_2O_7$?

Some defect interactions are perceivable in the investigated compositions, such as acceptor-vacancy association [1,20–22] and local vacancy-vacancy association due to high vacancy concentrations, as found in reduced ceria [23]. Depending on the strength of the association, the oxides could have oxygen vacancies with varying hydration affinities, determined by their local environment. Vacancies with endothermic hydration enthalpies will as such not hydrate and therefore lower the observed saturation level. Partial long-range order is found in the Nd-containing samples [17] and the oxygen ordering is, as we will discuss later, likely to stabilize the vacancies enough to efficiently inhibit hydration, but for now we will concentrate on the disordered fluorite structured $La_2Ce_2O_7$ (and the disordered fractions of the Nd-containing samples).

In a first approach, the limited hydration may be attempted rationalized by assigning a fraction of the vacancies to lower energies, i.e., that they are trapped in certain configurations of cations. If we assume that the structure is a disordered fluorite, both the oxygen and the cation sites are disordered, and each cation is on average 7-fold coordinated with oxygen, meanwhile each oxygen site is coordinated by four cations. Statistical analysis shows that an oxide with equal amounts of La^{3+} and Ce^{4+} like in $La_2Ce_2O_7$ ($x = 0$) has 16 different configurations of cations around each tetrahedrally coordinated oxide ion: The number of these configurations with 0, 1, 2, 3, and 4 La^{3+} ions is, respectively, 1, 4, 6, 4, and 1, summing up to 16. Of these, 2 are statistically vacant in $La_2Ce_2O_7$ (or $La_4Ce_4O_{14}$).

In this framework there is no way to assign any of these configurations with energetics for oxygen vacancies that give as limited hydration as observed. If we, for example, assume that one of the "end members" with either 4 La or 4 Ce coordinating the oxygen site trap oxygen vacancies strongly, this still leaves another vacancy available for hydration, corresponding to as much as 50% of the nominal amount – more than twice the experimental indication. If more of the 16 configurations trap oxygen vacancies, both vacancies will be trapped. If the trapping enthalpy is larger than the hydration enthalpy, they will remain unavailable for hydration and there will be no hydration. If the enthalpy is comparable or smaller, the hydration will however proceed and "unlock" the vacancies as temperature decreases or pH_2O increases, and the material will eventually hydrate fully.

Let us instead assume that one configuration – again one of the "end members" – has a favourably low energy for protons, i.e. acts as a strong trap for protons. Then hydration is limited to one proton per 16 oxide ion sites, which corresponds to one half water molecule – or half an oxygen vacancy filled. This is 25% of the 2 vacancies nominally available, which is strikingly close to the experimental indication of around 20%. A plausible "end member" site for these trapped protons is the oxygen site coordinated by 4 La^{3+} ions. While oxygen vacancies might have a slight preference for Ce^{4+} coordination or, vice versa, Ce^{4+} prefers oxygen vacancies because its small size favours low coordination numbers, the protonic defect may well neglect this aspect and instead be strongly attracted to the site surrounded by four of the basic lower valent La^{3+}.

We next show that the experimental water uptake of $La_2Ce_2O_7$ (or 50% La doped CeO_2) at pH_2O = 1 atm is well explained by the new model using rational parameters. It is herein assumed that all oxygen vacancies are free and unassociated with each other or any cation

configuration. Moreover, all hydration reactions are assigned a fitted standard entropy change of −108 J/mol K, well within what is normally found for reactions with loss of one molecule of gas, and hydration reactions in particular. In a first approach the hydration reaction is assigned a standard hydration enthalpy change of 0 for all oxygen sites except the 1 out of 16 which is assigned −64 kJ/mol of H_2O to fit the experimental data. This would mean that undoped CeO_2 is indifferent to hydration, but that the fully La-coordinated oxide ion traps protons with an enthalpy of −32 kJ/mol per proton. The model may hence equally well be represented by a general unfavourable hydration for the entire oxide, but with a proton trapping reaction to the La-coordinated site.

Indeed, CeO_2 is as such known not to hydrate, and DFT calculations have accordingly yielded a positive standard enthalpy of hydration for CeO_2 of +66 kJ/mol of H_2O [6]. If we take this enthalpy into the model for hydration of all sites except the fully La-coordinated one, we need a relatively more negative one for the fully La-coordinated one, i.e. a stronger trapping enthalpy now of the order of −70 kJ/mol per proton, to fit the experimental data. This is indeed in accordance with our preliminary ab initio DFT-calculations where we find an enthalpy difference of −70 kJ/mol for a proton on an oxide ion coordinated by 4 La^{3+} ions compared with 4 Ce^{4+} ions in a disordered fluorite $La_2Ce_2O_7$ lattice.

One may note that in the hydration reactions in the model applied, it does not matter which oxide ion site is filled with oxygen (the 4 La^{3+} coordinated one or any of the other ones) since they are per definition equal in this respect – it only matters where the protons end up.

The new model – whether it takes a CeO_2 with zero or positive hydration enthalpy as starting point – accounts for the main part of the modelled hydration, fitting qualitatively the measured hydration curve as well as the approach to the saturation level, as shown in Fig. 4. The upward tail at high temperatures is uncertain due to small hydration levels, but may reflect intermediate trapping energies for the less La-coordinated sites. The curve in Fig. 4 is indeed fitted with such a value for the 2 out of 16 sites with 1 Ce^{4+} + 3 La^{3+} coordination, yielding the hydration tail at higher temperatures due to the more favourable configurational entropy of 2 vs 1 out of 16 sites (see Fig. 4 caption for the exact parameters used in the modelled curve).

We note the qualitative agreement between the standard enthalpies of hydration of the order of approximately −64 kJ/mol of H_2O obtained here with the new model assuming zero hydration of CeO_2 and the −77 kJ/mol of H_2O obtained for $La_2Ce_2O_7$ by TG-DSC, as both represent apparent effective hydration of the material with limited saturation levels. However, as clear from the above, the knowledge of the endothermic hydration enthalpy of CeO_2 as such allows a more correct assessment of the enthalpies involved in the hydration (trapping of protons) to the dominating 4 La^{3+} site.

The trapping energy between a proton and an oxide ion coordinated by 4 Nd^{3+} is expected to be lower than for 4 La^{3+}, since the basicity of La is larger. This may explain the gradually decreasing negative apparent hydration enthalpy with increasing Nd-content from the TG-DSC results in this study (Table 1).

The present model points at a possibility that may have been overlooked in earlier works: The statistical variations of coordination around oxygen sites in a heavily doped oxide create a limited number of oxide ions with special properties, such as being so favourable sites for protons that an otherwise non-hydratable oxide displays a certain hydration. Applied to $La_2Ce_2O_7$ it means that 1/16 of the oxide ions may have this property and makes the material hydrate to 25% of the nominal acceptor (and oxygen vacancy) contents. It is interesting to note that the same principle then would be in effect also for less doped systems, but the resulting concentration of specially coordinated oxygen sites to be protonated would be drastically reduced. For instance, 1 and 10 mol% La-doped CeO_2 would have only $1 \cdot 10^{-8}$ and $1 \cdot 10^{-4}$ of the oxygen sites coordinated by 4 La^{3+} ions, resulting in the same numbers of H_2O per mole of CeO_2, in turn representing hydration of merely 2 ppm and 0.2% of the oxygen vacancies, which would easily pass unnoticed.

In general, the degree of hydration F_{hydr} from a complete coordination of an acceptor cation Acc in an oxide MO_b where the oxide ions are coordinated by a number C of cations M is according to our simple considerations expressed as

$$F_{hydr} = \frac{[H_2O]}{[v_O^{\bullet\bullet}]} = \frac{\frac{[OH_O^{\bullet}]}{2}}{[v_O^{\bullet\bullet}]} = \frac{\frac{[O_{coord}]}{2}}{[v_O^{\bullet\bullet}]} = \frac{\frac{bX_{O_{coord}}}{2}}{[v_O^{\bullet\bullet}]} = \frac{\frac{b[Acc_M^{/}]^C}{2}}{\frac{[Acc_M^{/}]}{2}} = \frac{b[Acc_M^{/}]^C}{[Acc_M^{/}]} = b[Acc_M^{/}]^{C-1} \quad (6)$$

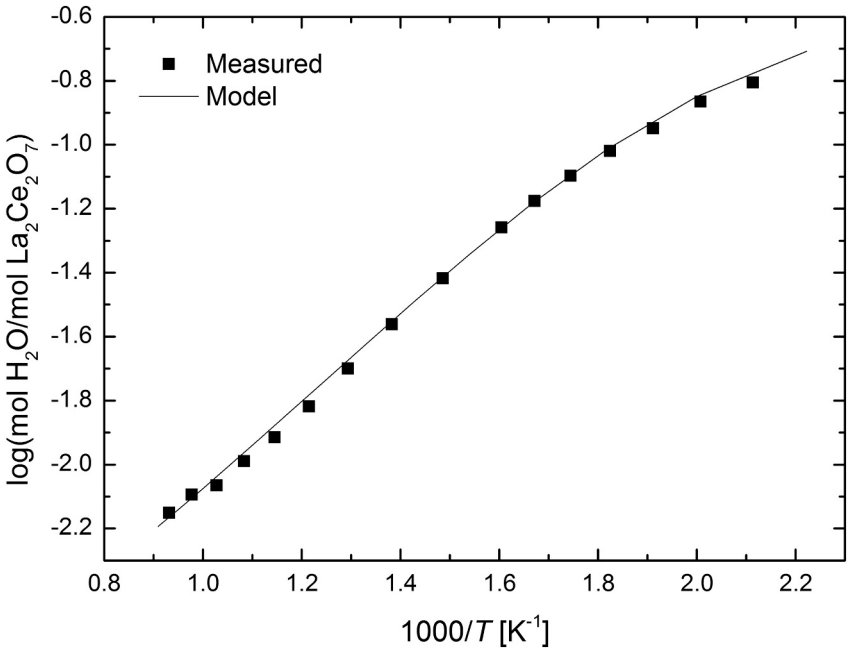

Fig. 4. Measured water uptake in $La_2Ce_2O_7$ vs 1000/T compared with modelled values, explained in the text, using standard entropy and enthalpy of hydration of, respectively, −108 J/mol K and +66 kJ/mol of H_2O, and trapping enthalpies of protons to the 1/16 sites coordinated by 4 La^{3+} and 2/16 sites coordinated by 1 Ce^{4+} + 3 La^{3+} of, respectively −65 and − 47 kJ/mol of protons.

where square parentheses denote molar fraction and X denotes site fraction. The number 2 emerges simply from electroneutrality and valence considerations of protons vs oxide ions. For fluorite oxides MO_2, $b = 2$ and $C = 4$, yielding the numbers calculated above. For perovskites AMO_3 doped on the M-site, $b = 3$ and $C = 2$. For instance, 10% doping of a very basic acceptor on the M-site of a perovskite with otherwise unfavourable hydration thermodynamics could be hydrated to 30% of the nominal level. This big effect for perovskites stems from the oxygen coordination C being as low as 2 in this case, and reminds us that the expression fails for cases predicting $F_{hydr} > 1$, which would be at > 33% acceptor doping for perovskites. Real cases of oxides with more favourable hydration thermodynamics will obviously reflect protonation of oxide ions of various coordination, yielding intermediate full hydration levels and apparent thermodynamic parameters.

Concluding this part we repeat the argument that stabilization of protons on oxide ions largely coordinated to basic acceptor dopants yields the dominating energy that enables hydration in the disordered fluorite, while it at the same time then may limit the amount of hydration well below the nominal one expected from the acceptor doping level.

3.3. Effect of vacancy ordering on hydration

Fig. 5 shows the actual water uptake as a function of x in $La_{2-x}Nd_xCe_2O_7$ for different temperatures (connected symbols) and the estimated maximum uptake - saturation values – from fitting the water uptake (dashed line) according to the standard hydration model for a variable content of effective acceptors and free vacancies. The actual as well as the maximum water uptakes are decreasing considerably with increasing x. We will here explore this in terms of the effect of long-range vacancy order.

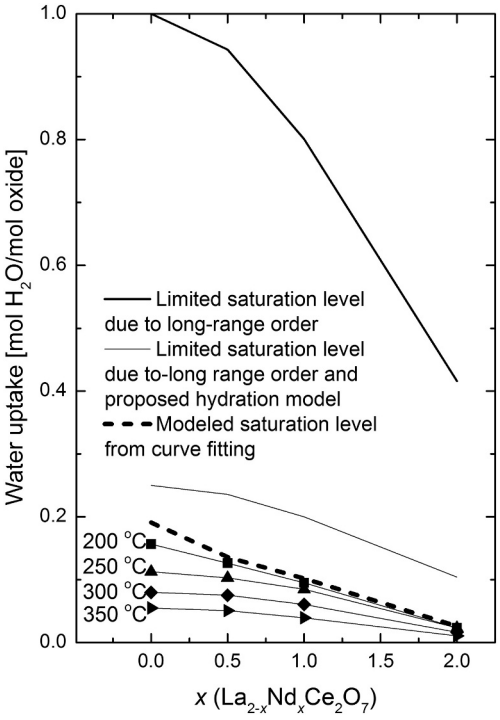

Fig. 5. The water uptake at 1 atm H_2O measured at different temperatures as function of composition ($La_{2-x}Nd_xCe_2O_7$ x = 0, 0.5, 1 and 2) as well as the estimated saturation level according to the degree of long-range order (thick solid line) and estimated saturation level based on the proposed models for limitations of hydration on both the disordered and ordered fractions (thin solid line) and the saturation level obtained by curve fitting of the water uptake data (dashed line).

In addition to the aforementioned local association forces between protons and La/Nd, we also have to consider long-range order in this compositional series. Our previous work on these compositions shows that $La_2Ce_2O_7$ is best described by the defect fluorite structure where the cations and oxygen vacancies are disordered [17]. The other end member, $Nd_2Ce_2O_7$, was shown to adopt a C-type structure with oxygen excess for more than 50% of the volume, while the other half adopted a defect fluorite structure [17]. Thus, there is an increasing tendency for partial long-range vacancy order as the Nd-content increases. The structural relaxation stabilizing the whole lattice during ordering effectively stabilizes the vacancies, making them harder, or impossible, to hydrate. This can therefore explain a further decrease in the observed water uptake and saturation level with increasing Nd-content in the composition, in correspondence with the measured TG data (cf. Fig. 5).

Based on this we rationalize the observed trends, for the sake of simplicity and illustration, by dividing the matrix of each composition containing Nd, into two parts;

1) a part of the volume having a disordered lattice only offering a fraction of hydration due to different local environments of host and acceptor dopant cations, as discussed above, and
2) a remaining part having a dominant long-range order between vacancies inhibiting both mobility and hydration.

The amount of the latter type of lattice increases with Nd content. We have used input from the structural investigations and estimated the relative amount of long-range order across the material series. By subtracting the amount of oxide related to the observed long-range order, we obtain an estimate of the remaining part of the oxide which is available for hydration, represented by the top thick black line in Fig. 5. Now assuming that only 25% of these free vacancies hydrate under the present conditions, we have calculated how the saturation level is expected to change across the $La_{2-x}Nd_xCe_2O_7$ series. We used $La_2Ce_2O_7$ ($x = 0$) as the starting point, where no long-range order has been observed, with a hydration saturation level of 0.25, and the estimated hydration level decreases as x and long-range order evolve (included in Fig. 5 as the thin black line). Although this does not reproduce the fitted saturation levels (dashed lines) completely, it qualitatively corresponds with the overall trend in the behaviour of the experimental data. The fact that the apparent level of saturation decreases with increasing Nd content is in line with this simple estimation, including both of the proposed models for limitations in the disordered and the ordered fractions of the sample.

The discrepancy between the estimated saturation level resulting from the combined model of long-range vacancy order and short range proton trapping (thin black line) and the saturation estimated from our measurements can be explained by additional locking of vacancies due to local vacancy association of the same type as giving long-range order. Such vacancy association occurs as pairs or clusters even in $La_2Ce_2O_7$ to some small degree, but will not be observed by diffraction (see previous work for elaboration [17]).

3.4. Correlations with electrical conductivity

The conductivity of all the samples, except $La_2Ce_2O_7$, increases with pO_2 in oxidizing atmospheres, more pronounced with increasing Nd content. This reflects p-type electronic conductivity from minority electron holes, which generally speaking can be ascribed to the slight tendency of Nd^{3+} to be oxidized to Nd^{4+}, evidenced also in previous work on $Nd_2Ce_2O_7$ [15]. Studies of oxide ion and protonic conductivity are hence done in Ar atmospheres, where the p-type conductivity is negligible.

Fig. 6 (left) shows the conductivity vs pH_2O for water levels up to ~2.5%. The conductivity increases with increasing water vapour and the effect increases with decreasing temperature, according to the exothermic hydration enthalpy. Moreover, the effects of water vapour

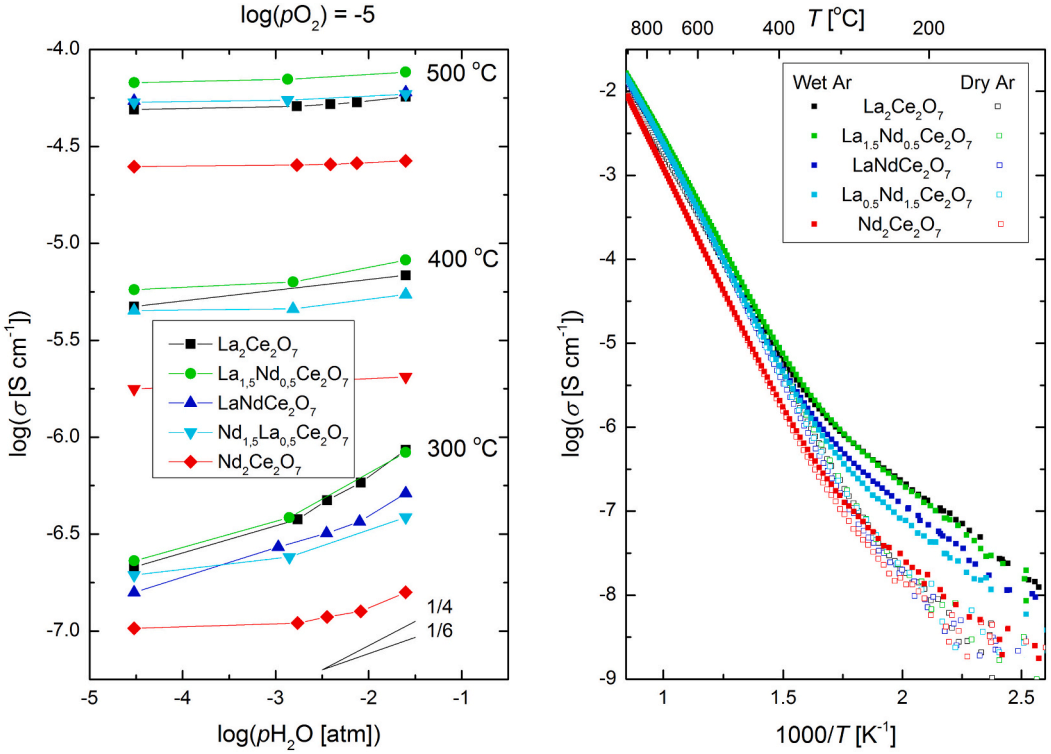

Fig. 6. Left: Isothermal conductivities in Argon with increasing pH_2O. Right: Isobaric conductivities in wet and dry Argon.

are stronger for the La-rich compositions. These observations are supporting the above discussion. Notably, the dependencies never reach neither the expected $pH_2O^{1/2}$ dependencies nor saturation, as the water vapour pressures are two orders of magnitude lower than the 1 atm used in the TG-DSC measurements and the temperatures are well higher than the saturation range.

Fig. 6 (right) shows the temperature dependencies in wet Ar. At high temperatures oxide ion conductivity predominates with apparent activation energies for $La_2Ce_2O_7$ increasing from 95 kJ/mol at the highest temperatures to around 103 kJ/mol at intermediate temperatures. This slightly non-linear Arrhenius-like behaviour may reflect a small tendency of association or local order. With increasing Nd contents, the activation energy increases further, to around 116 kJ/mol for $Nd_2Ce_2O_7$, in line with the increasing oxygen vacancy ordering.

At low temperatures the protonic contribution becomes dominating, in agreement with previous work [2,14,15]. Fitting the straight portions yields activation energies for proton conductivity increasing monotonously from around 43 kJ/mol for $La_2Ce_2O_7$ to around 50 kJ/mol for $Nd_2Ce_2O_7$. Assuming equilibrium in the minor proton concentration given by the trapping to specific sites, and that the mobility of protons is limited by untrapping and by free proton migration between traps, the effects of trapping on conductivity cancel, and the observed enthalpy will reflect only jumps of free untrapped protons, hence being 43 kJ/mol in $La_2Ce_2O_7$ and 50 kJ/mol in $Nd_2Ce_2O_7$ based on our measurements. The activation energies for conductivity and hence mobility of untrapped protons this way come out as roughly half that for oxygen vacancies in these materials.

4. Conclusions

The system $La_{2-x}Nd_xCe_2O_7$ (x = 0, 0.5, 1 and 2) displays a cubic disordered structure corresponding to 50% La-doped CeO_2 for $La_2Ce_2O_7$ (x = 0) and with more oxygen vacancy ordering as x increases [17]. $La_2Ce_2O_7$, or 50% La-doped CeO_2, hydrates, despite the fact that the moderately acceptor doped parent oxide CeO_2 does not. The hydration decreases with increasing Nd content x.

The amount and enthalpy of hydration of $La_{2-x}Nd_xCe_2O_7$ (x = 0, 0.5, 1 and 2) have been measured using TG-DSC. The observed hydration is far from the theoretical limit corresponding to 50 mol% acceptor doped ceria. We suggest herein a new model in which the statistical variation of coordination around oxygen sites in a heavily doped fluorite oxide creates a limited number of oxide ion sites that favour incorporation of a proton. If for instance only the one oxygen site coordinated by 4 La^{3+} ions in $La_2Ce_2O_7$ is protonated, this corresponds to hydration of only ¼ (25%) of the oxygen vacancies, close to the experimentally observed saturation limit. The hydration enthalpies for $La_{2-x}Nd_xCe_2O_7$ are found to be in the range − 77 to −71 kJ/mol based on the TG-DSC data, becoming slightly less exothermic with increasing Nd-content. The fitting of the TG data to a model of protonation of only statistically fully La^{3+} coordinated oxygen sites yields a proton bonding energy to this site of around −32 kJ/mol (corresponding to a hydration enthalpy for this site of −64 kJ/mol) for $La_2Ce_2O_7$ if the we assume a hydration enthalpy equal to 0 for the host compound CeO_2 otherwise. However, if we assume that CeO_2 has an unfavourably endothermic enthalpy of hydration (e.g. +66 kJ/mol H_2O based on DFT), a correspondingly stronger trapping of protons to the 4 La^{3+} coordinated oxide ion is required to fit the experimental data, e.g. close to −70 kJ/mol per proton.

Less La^{3+} coordinated oxide ions may have intermediate proton trapping energies, as indicated by our data also. The new model may be generally applicable to hydration of other heavily doped oxides with otherwise unfavourable hydration, and explain cases of hydration far from the nominal.

The proton conductivity exhibits an activation energy of 43 kJ/mol

for $La_2Ce_2O_7$ increasing to 50 kJ/mol for $Nd_2Ce_2O_7$ under conditions with minority proton concentrations, which then corresponds to the activation energy for mobility of free untrapped protons.

The observed decrease in water uptake with increasing Nd content x is interpreted to reflect an increasing tendency to long-range order that inhibits hydration of an increasing fraction of the vacancies.

Credit author statement

Liv-Elisif Kalland: Conceptualization, Methodology, Formal Analysis, Investigation, Writing - Original Draft, Writing –Review & Editing
Andreas Løken: Methodology, Formal Analysis, Writing – Review & Editing
Tor Bjørheim: Methodology, Formal Analysis, Writing – Review & Editing
Reidar Haugsrud: Conceptualization, Writing – Review & Editing, Supervision
Truls Norby: Conceptualization, Methodology, Writing - Original Draft (minor parts), Writing – Review & Editing, Supervision.

Declaration of competing interest

The authors declare that they have no known competing financial interests or personal relationships that could have appeared to influence the work reported in this paper.

Acknowledgements

The computations were performed on resources provided by UNINETT Sigma2 – the National Infrastructure for High Performance Computing and Data Storage in Norway.

References

[1] D.Y. Wang, D.S. Park, J. Griffith, A.S. Nowick, Solid State Ionics 2 (2) (1981) 95.
[2] V. Besikiotis, C.S. Knee, I. Ahmed, R. Haugsrud, T. Norby, Solid State Ionics 228 (2012) 1.
[3] T. Hagiwara, Z. Kyo, A. Manabe, H. Yamamura, K. Nomura, J. Ceram, Soc. Jpn. 117 (Dec.) (2009) 1306.
[4] T.S. Bjørheim, A. Løken, R. Haugsrud, J. Mater. Chem. A 4 (16) (2016) 5917.
[5] T. Norby, M. Wideroe, R. Gloeckner, Y. Larring, Dalton Trans. (2004) 3012.
[6] T. Zacherle, A. Schriever, R.A. De Souza, M. Martin, Phys. Rev. B 87 (13) (2013) 134104.
[7] R. Haugsrud, Y. Larring, T. Norby, Solid State Ionics 176 (39–40) (2005) 2957.
[8] Y. Larring, T. Norby, Solid State Ionics 97 (1–4) (1997) 523.
[9] T.S. Bjørheim, V. Besikiotis, R. Haugsrud, Dalton Trans. 41 (43) (2012) 13343.
[10] K.D. Kreuer, Annu. Rev. Mater. Res. 33 (2003) 333.
[11] C. Kjølseth, L.-Y. Wang, R. Haugsrud, T. Norby, Solid State Ionics 181 (39) (2010) 1740.
[12] J. Faber, C. Geoffroy, A. Roux, A. Sylvestre, P. Abélard, Appl. Phys. A Solids Surf. 49 (3) (1989) 225.
[13] H. Yahiro, Y. Eguchi, K. Eguchi, H. Arai, J. Appl. Electrochem. 18 (4) (1988) 527.
[14] W. Sun, S. Fang, L. Yan, W. Liu, Fuel Cells 12 (3) (2012) 457.
[15] S. Cheng. Master thesis, Department of Physics, University of Oslo, Oslo (2012).
[16] Z.G. Liu, J.H. Ouyang, K.N. Sun, Fuel Cells 11 (2) (2011) 153.
[17] L.-E. Kalland, S.T. Norberg, J. Kyrklund, S. Hull, S.G. Eriksson, T. Norby, C.E. Mohn, C.S. Knee, Phys. Chem. Chem. Phys. 18 (34) (2016) 24070.
[18] A. Løken, T.S. Bjørheim, R. Haugsrud, J. Mater. Chem. A 3 (46) (2015) 23289.
[19] K.D. Kreuer, S. Adams, W. Münch, A. Fuchs, U. Klock, J. Maier, Solid State Ionics 145 (1) (2001) 295.
[20] V. Butler, C.R.A. Catlow, B.E.F. Fender, J.H. Harding, Solid State Ionics 8 (2) (1983) 109.
[21] L. Minervini, M.O. Zacate, R.W. Grimes, Solid State Ionics 116 (3–4) (1999) 339.
[22] R. Gerhardt-Anderson, A.S. Nowick, Solid State Ionics 5 (1981) 547.
[23] S. Hull, S.T. Norberg, I. Ahmed, S.G. Eriksson, D. Marrocchelli, P.A. Madden, J. Solid State Chem. 182 (10) (2009) 2815.